Rapid Communications | Editors' Suggestion

Experimental observation of Dirac cones in artificial graphene lattices

Shaosheng Yue,[1,3] Hui Zhou,[1,3] Daiyu Geng,[1,3] Zhenyu Sun,[1,3] Masashi Arita,[2] Kenya Shimada,[2] Peng Cheng,[1,3] Lan Chen,[1,3,4] Sheng Meng,[1,3,*] Kehui Wu,[1,3,4,†] and Baojie Feng[1,3,‡]

[1]*Institute of Physics, Chinese Academy of Sciences, Beijing 100190, China*

[2]*Hiroshima Synchrotron Radiation Center, Hiroshima University, 2-313 Kagamiyama, Higashi-Hiroshima 739-0046, Japan*

[3]*School of Physical Sciences, University of Chinese Academy of Sciences, Beijing 100049, China*

[4]*Songshan Lake Materials Laboratory, Dongguan, Guangdong 523808, China*

(Received 21 July 2020; accepted 30 September 2020; published 9 November 2020)

Artificial lattices provide a tunable platform to realize exotic quantum devices. A well-known example is artificial graphene (AG), in which electrons are confined in honeycomb lattices and behave as massless Dirac fermions. Recently, AG systems have been constructed by manipulating molecules using scanning tunneling microscope tips, but the nanoscale sizes typical for these constructed systems are impossible for practical device applications and insufficient for direct investigation of the electronic structures using angle-resolved photoemission spectroscopy (ARPES). Here, we demonstrate the synthesis of macroscopic AG by the self-assembly of C_{60} molecules on metal surfaces. Our theoretical calculations and ARPES measurements directly confirm the existence of Dirac cones at the K (K') points of the Brillouin zone, in analogy to natural graphene. These results will stimulate ongoing efforts to explore the exotic properties in artificial lattices and provide an important step forward in the realization of molecular quantum devices.

DOI: 10.1103/PhysRevB.102.201401

Graphene is a single layer of carbon atoms with a honeycomb lattice, and it has been intensively studied in the past decade [1,2]. In proximity to the Fermi level, the electrons in graphene behave as massless Dirac fermions. This is the origin of graphene's various exotic properties, such as half-integer quantum Hall effects [3,4] and the Klein paradox [5–7]. An alternative way to realize the exotic properties of graphene is by confining the electrons of a two-dimensional electron gas (2DEG) to an equivalent honeycomb lattice, called artificial graphene (AG) [8–10]. Because of the confinement, there exists a Dirac cone at each K point of the Brillouin zone (BZ). As a result, electrons of the otherwise 2DEG behave as massless Dirac fermions, which is analogous to the case of natural graphene. In addition to possessing the novel properties of graphene, artificial lattices possess various tunable parameters, thereby providing an ideal platform for the simulation of quantum behaviors in two-dimensional (2D) Dirac materials [11–15].

Some molecules, such as carbon monoxide and coronene, can serve as potential barriers through which the electrons of the 2DEG are forbidden to travel. Therefore, a hexagonally patterned molecular lattice can confine the 2DEG electrons into an equivalent honeycomb lattice and lead to the realization of AG [8,9], as illustrated in Figs. 1(a) and 1(b). In 2012, Gomes *et al.* constructed the first AG by atomic manipulation of carbon monoxide molecules on Cu(111) and found experimental evidence of massless Dirac fermions by scanning tunneling spectroscopy [8]. In addition to the scheme presented by molecular AG, AG has also been realized in nanopatterned GaAs quantum wells [16–18]. Unlike unpatterned GaAs quantum wells, resonant inelastic light-scattering spectra of the AG system revealed low-lying transitions that might arise from the Dirac bands [18]. The high energy and momentum resolution of angle-resolved photoemission spectroscopy (ARPES) makes it a powerful technique to directly study the electronic structures of materials. However, a direct experimental observation of the Dirac cones in AG using ARPES has yet to be reported.

Here, we constructed macroscopic AG systems by growing monolayer C_{60} molecules on the (111)-terminated surfaces of noble metals, which enabled ARPES studies of the electronic band structure. Our low-energy electron diffraction (LEED) and ARPES measurements show that these AG systems are homogeneous. Therefore, their size is only limited by the scale of the substrates. The Dirac cones at the K (K') points were directly observed by our ARPES measurements. In addition, we performed model calculations on these AG systems, whose results fully supported our experimental observations.

The lattice constant of nanopatterned structures is typically tens of hundreds of nanometers, which is several orders of magnitude larger than that of conventional single crystals [16–18]. Such a large lattice constant results in a very small BZ that is beyond the resolution of conventional ARPES facilities. The molecular AG system is ideal for the investigation of electronic structures because of its moderate lattice constants. However, the size of conventional AG systems constructed by atomic/molecular manipulation is limited to the nanoscale, which is typically insufficient for practical device applications and for electronic band-structure investigations. A promising

*smeng@iphy.ac.cn
†khwu@iphy.ac.cn
‡bjfeng@iphy.ac.cn

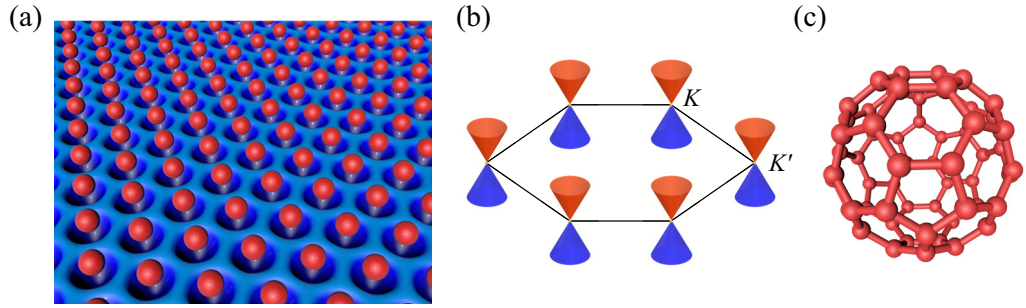

FIG. 1. Schematic of artificial graphene (AG). (a) Molecular AG system, including molecules that act as potential barriers for electrons (red balls) and the electron density profile (blue surfaces). Because of the presence of hexagonally patterned molecules, electrons of the otherwise two-dimensional electron gas are confined in a honeycomb lattice. (b) Band structure of AG. A Dirac cone exists at the K (K') point of the Brillouin zone (BZ), as an analogy to graphene. (c) Structure model of a C_{60} molecule. The nearly isotropic shape of C_{60} makes it an ideal choice for the construction of AG.

route to realize macroscopic AG is by preparing a molecular self-assembled monolayer on a metal substrate, where such supramolecular architectures can be well ordered across the entire substrate surface. A particular interesting molecule is C_{60}, which has a nearly isotropic spherical shape, as shown in Fig. 1(c). Previous works have shown that C_{60} molecules can form hexagonal structures on various noble metal surfaces, including Cu(111), Au(111), and Ag(111). In these systems, the electrons of the 2DEG of the metal surfaces are confined in an equivalent honeycomb lattice and are thus expected to behave as massless Dirac fermions.

First, we studied C_{60} monolayers on Cu(111). The C_{60} molecules form a hexagonal structure with a 4×4 superstructure with respect to the 1×1 lattice of Cu(111) [19,20]. The low-energy electron diffraction (LEED) patterns of the C_{60} monolayer on Cu(111) are shown in Fig. S1 [21]. The BZs of the C_{60} monolayer and of Cu(111) are schematically drawn in Fig. 2(a). Based on the above discussion, this system is expected to be an AG with a lattice constant of 10 Å. Figure 2(b) shows the ARPES intensity of the Fermi surface. The Shockley surface state of Cu(111) almost disappears because of the coverage of the C_{60} molecules. Instead, a dotlike spectral weight can be seen at each K (K') point. Such features do not exist on pristine Cu(111) because pristine Cu(111) only exhibits Shockley surface states at the BZ center and bulk sp bands at the BZ boundary. At deeper binding energies, the dots

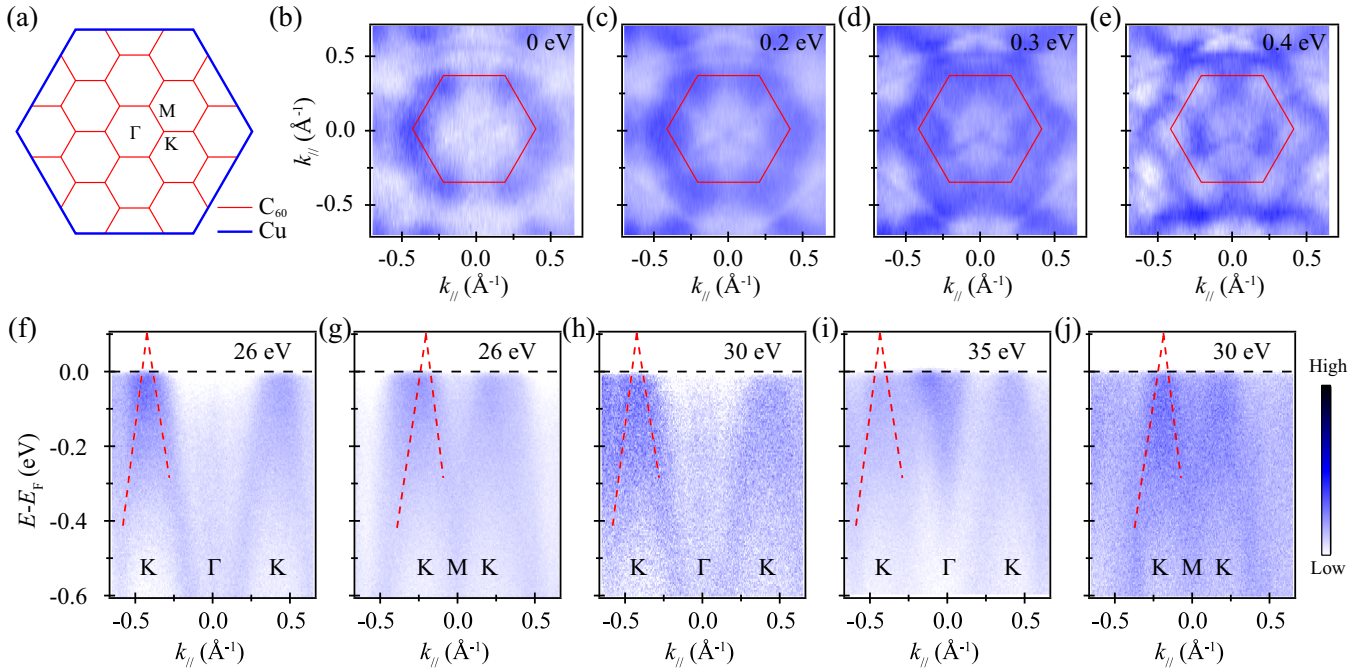

FIG. 2. ARPES measurements of the C_{60} monolayer on Cu(111). (a) Schematic of the BZs of the C_{60} monolayer (red) and Cu(111) (blue). C_{60} forms a 4×4 superstructure with respect to the 1×1 lattice of Cu(111). (b)–(e) ARPES intensity maps of the constant energy contours at different binding energies: (b) 0, (c) 0.2, (d) 0.3, and (e) 0.4 eV. Red hexagons indicate the BZs of the monolayer C_{60}. (f), (g) ARPES intensity plots along the (f) K-Γ-K and (g) K-M-K directions. The incident photon energy is 26 eV. (h), (i) ARPES intensity plots of the band structures along the K-Γ-K direction measured with the photon energy of (h) 30 and (i) 35 eV. (j) ARPES intensity plot along the K-M-K direction measured with the photon energy of 30 eV. Red dotted lines indicate the Dirac cone at the K point of the BZ and are guides for the eye.

become circles and their size increases as the binding energies increase, as shown in Figs. 2(c)–2(e).

Figure 2(f) shows the ARPES spectra along the Γ-K direction. One can observe linearly dispersing bands at the K point, as indicated by the red dashed lines. The fitted crossing point is located approximately 0.1 eV above the Fermi level. Along the K-M-K direction, the dispersion of the bands is also linear, as shown in Fig. 2(g). Combined with the evolution of the constant energy contours, we can conclude that there is a Dirac cone at each K point. The Dirac point is located above the Fermi level, and therefore the upper portion of the Dirac cone is inaccessible by conventional ARPES. The upward shift of the Dirac point may originate from the high electron affinity of the C_{60} molecules, which leads to a significant charge transfer from the substrate to the C_{60} molecules [22]. The Fermi velocity along the Γ-K direction is approximately 4×10^5 m/s, which is slightly smaller than that of natural graphene. In addition, the Dirac bands do not disperse with different photon energies, as shown in Figs. 2(h)–2(j), which agrees with their 2D character. Therefore, the ARPES results confirm that the C_{60}/Cu(111) system is an AG with Dirac cones at the K (K') points of the BZ.

We then performed a model analysis to understand the physics of the AG system. We note that the Cu(111) surface hosts Shockley-type surface states inside an inverted energy gap at the center of the BZ, and is thus a model 2DEG system. This is the reason for the success in the construction of AG by atomic/molecular manipulation [8,9]. The Hamiltonian of a 2DEG can be described as

$$H_0 = -\frac{\hbar^2\nabla^2}{2m^*}, \tag{1}$$

where m^* is the electron effective mass, $\hbar$ the reduced Planck constant, and ∇ the vector differential operator. For the Cu(111) surface, m^* is approximately $0.38m_e$. The eigenvalues and eigenstates can be determined using $E(k) = \hbar^2k^2/2m^*$ and $\psi = e^{ikr}/\sqrt{\Omega}$, where Ω is the volume of the primitive cell, k the electron momentum, and r the electron position. To simplify the analysis, we used a periodic potential $U(r)$ to simulate the effects of the C_{60} monolayer. The Hamiltonian of the modulated 2DEG can be given as

$$H = H_0 + U(r) = -\frac{\hbar^2\nabla^2}{2m^*} + \sum_{G_\alpha} U_{G_\alpha} e^{iG_\alpha\cdot r}, \tag{2}$$

where G_α ($\alpha = 1, 2, \ldots, 6$) are the six nearest reciprocal lattice vectors. To simplify the analysis, the C_{60} molecule can be treated as an isotropic sphere. Therefore, the C_{60}/Cu(111) system possesses C_6 symmetry and all U_{G_α} should be equal, i.e., $U_{G_1} = U_{G_2} = U_{G_3} = U_{G_4} = U_{G_5} = U_{G_6} = U_0$. As a result, the band structures of the system can be solved numerically. When the interaction between C_{60} and Cu(111) is turned off, the parabolic bands of 2DEG are simply folded into the BZ of the C_{60} superstructure, as shown in Fig. 3(a). With a proper U_0 value such as 0.4 eV, the Dirac cone at the K (K') point emerges and resembles that of natural graphene, as shown in Fig. 3(b). The calculated Fermi velocity along the Γ-K direction is approximately 6.27×10^5 m/s, which is close to the experimental value (4×10^5 m/s). It should be noted that the calculated Fermi velocity of the Dirac cone is insensitive to the variation of U_0 [see Supplemental Material, Supplemental Eqs. (E1)–(E8) and Fig. S2 for details [21]].

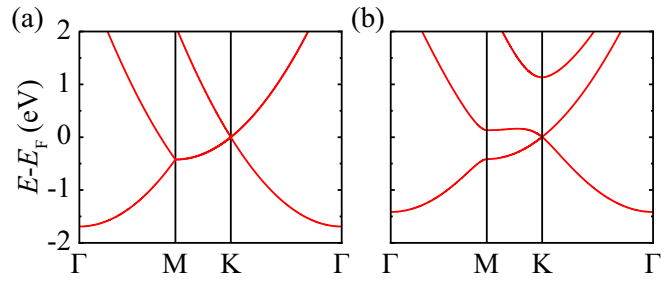

FIG. 3. Model analysis of artificial graphene. (a), (b) Calculated band structures for (a) $U_0 = 0$ eV and (b) $U_0 = 0.4$ eV.

The success of realizing AG in the C_{60}/Cu(111) system provides a universal method for the realization of AG using other noble metal substrates. Another prototypical 2DEG system is Au(111), on which C_{60} molecules can also form ordered monolayer structures [23–25]. Because of the larger lattice constant of Au(111) ($a_{Au} = 2.9$ Å) compared with that of Cu(111) ($a_{Cu} = 2.5$ Å), the C_{60} molecules form a $2\sqrt{3}\times2\sqrt{3}$ superstructure with respect to the 1×1 lattice of Au(111). This different superstructure provides further evidence for the universality of this method. As expected, our ARPES results show the existence of Dirac cones at each K (K') point of the BZ, as shown in Figs. 4(b) and 4(c). The Dirac bands do not disperse with varying photon energy, which again agrees with their 2D character. In addition, the Dirac point of the C_{60}/Au(111) system is located approximately 0.2 eV below the Fermi level, and therefore the upper Dirac cone can be observed by our ARPES measurements. The higher binding energy of the Dirac point in the C_{60}/Au(111) system may originate from the smaller charge transfer from the substrate to C_{60}. This is reasonable because the electron affinity of gold is higher than that of copper. The Fermi velocity along the Γ-K direction is approximately 1.2×10^6 m/s, which is slightly higher than that of natural graphene.

Finally, we discuss possible device applications based on these AG systems. First, Cu and Au are commonly used conducting materials, such as electrodes. After depositing a monolayer C_{60}, the emergence of 2D Dirac fermions enable the realization of Klein tunneling [5–7], that is, the electrons pass unimpeded through potential barriers. This is a crucial component in fabricating low-dissipation quantum devices. Second, noble metals, including Au and Cu, are well-known plasmonic materials with a strong visible light response [26]. The emergence of 2D Dirac fermions on noble metal surfaces indicates the possibility of realizing Dirac plasmons [27,28] in the visible light region, which can be widely used in optoelectronic devices. Notably, plasmonic devices with a visible light response are difficult to realize using natural graphene.

All of our results support the realization of AG in the self-assembled C_{60} monolayer on noble metal surfaces. The Dirac cones at the K (K') points of the BZ are directly observed by our ARPES measurements. The realization of AG in molecular self-assembled monolayers offers great opportunities for the fabrication of exotic molecular quantum devices.

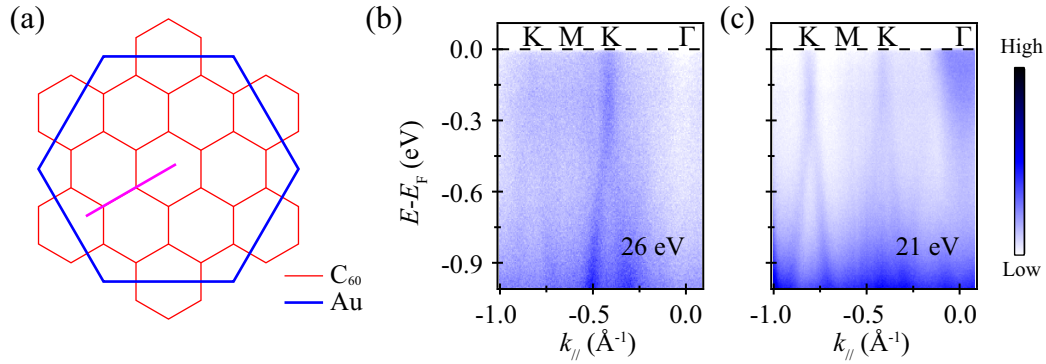

FIG. 4. ARPES measurements of the C_{60} monolayer on Au(111). (a) Schematic of the BZs of the C_{60} monolayer (red) and Au(111) (blue). The pink line indicates the momentum direction of the cuts in (b) and (c). (b), (c) ARPES intensity plots along the Γ-*K*-*M*-*K* direction using incident photon energies of (b) 26 and (c) 21 eV. The Dirac cone at the *K* point can be clearly observed. The Dirac point is located approximately 0.2 eV below the Fermi level.

Because of the high tunability of supramolecular architectures, such molecular AG systems can also enable the investigation of Dirac fermions under various conditions, such as doping and symmetry breaking, by choosing appropriate molecules, dopants, and substrates. It should be noted that the bulk and thin film of C_{60} will become a high-temperature superconductor with appropriate alkali metal doping [29–31]. Therefore, it is highly anticipated that the doped C_{60} monolayer will host rich physics that originate from the interplay between Dirac fermions and superconductivity; these interesting properties can be probed by various experimental techniques, such as transport, scanning tunneling spectroscopy, and ARPES.

This work was supported by the Ministry of Science and Technology of China (Grant No. 2018YFE0202700), the National Natural Science Foundation of China (Grants No. 11974391, No. 11825405, No. 1192780039, No. 11761141013), the Beijing Natural Science Foundation (Grant No. Z180007), and the Strategic Priority Research Program of the Chinese Academy of Sciences (Grants No. XDB33030100 and No. XDB30000000). The synchrotron ARPES measurements were performed with the approval of the Proposal Assessing Committee of Hiroshima Synchrotron Radiation Center (Proposals No. 19BG007 and No. 19BG028).

S.Y. and H.Z. contributed equally to this work.

[1] A. K. Geim and K. S. Novoselov, The rise of graphene, Nat. Mater. **6**, 183 (2007).
[2] A. H. Castro Neto, F. Guinea, N. M. R. Peres, K. S. Novoselov, and A. K. Geim, The electronic properties of graphene, Rev. Mod. Phys. **81**, 109 (2009).
[3] K. S. Novoselov, A. K. Geim, S. V. Morozov, D. Jiang, M. I. Katsnelson, I. V. Grigorieva, S. V. Dubonos, and A. A. Firsov, Two-dimensional gas of massless Dirac fermions in graphene, Nature (London) **438**, 197 (2005).
[4] Y. Zhang, J. W. Tan, H. L. Stormer, and P. Kim, Experimental observation of the quantum Hall effect and Berry's phase in graphene, Nature (London) **438**, 201 (2005).
[5] M. I. Katsnelson, K. S. Novoselov, and A. K. Geim, Chiral tunnelling and the Klein paradox in graphene, Nat. Phys. **2**, 620 (2006).
[6] A. F. Young and P. Kim, Quantum interference and Klein tunnelling in graphene heterojunctions, Nat. Phys. **5**, 222 (2009).
[7] C. Gutiérrez, L. Brown, C.-J. Kim, J. Park, and A. N. Pasupathy, Klein tunnelling and electron trapping in nanometre-scale graphene quantum dots, Nat. Phys. **12**, 1069 (2016).
[8] K. K. Gomes, W. Mar, W. Ko, F. Guinea, and H. C. Manoharan, Designer Dirac fermions and topological phases in molecular graphene, Nature (London) **483**, 306 (2012).
[9] S. Wang, L. Z. Tan, W. Wang, S. G. Louie, and N. Lin, Manipulation and Characterization of Aperiodical Graphene Structures Created in a Two-Dimensional Electron Gas, Phys. Rev. Lett. **113**, 196803 (2014).
[10] M. Nantoh, K. Takashima, T. Yamamoto, and K. Ishibashi, Sublattice site dependence of local electronic states in superstructures of CO built on a Cu(111) surface, Phys. Rev. B **96**, 035424 (2017).
[11] A. Singha, M. Gibertini, B. Karmakar, S. Yuan, M. Polini, G. Vignale, M. I. Katsnelson, A. Pinczuk, L. N. Pfeiffer, K. W. West, and V. Pellegrini, Two-dimensional Mott-Hubbard electrons in an artificial honeycomb lattice, Science **332**, 1176 (2011).
[12] L. Tarruell, D. Greif, T. Uehlinger, G. Jotzu, and T. Esslinger, Creating, moving and merging Dirac points with a Fermi gas in a tunable honeycomb lattice, Nature (London) **483**, 302 (2012).
[13] M. Polini, F. Guinea, M. Lewenstein, H. C. Manoharan, and V. Pellegrini, Artificial honeycomb lattices for electrons, atoms and photons, Nat. Nanotechnol. **8**, 625 (2013).
[14] S. N. Kempkes, M. R. Slot, J. J. van den Broeke, P. Capiod, W. A. Benalcazar, D. Vanmaekelbergh, D. Bercioux, I. Swart, and C. M. Smith, Robust zero-energy modes in an electronic higher-order topological insulator, Nat. Mater. **18**, 1292 (2019).

[15] S. N. Kempkes, M. R. Slot, S. E. Freeney, S. J. M. Zevenhuizen, D. Vanmaekelbergh, I. Swart, and C. M. Smith, Design and characterization of electrons in a fractal geometry, Nat. Phys. **15**, 127 (2019).

[16] M. Gibertini, A. Singha, V. Pellegrini, and M. Polini, Engineering artificial graphene in a two-dimensional electron gas, Phys. Rev. B **79**, 241406(R) (2009).

[17] S. Wang, D. Scarabelli, Y. Y. Kuznetsova, S. J. Wind, A. Pinczuk, V. Pellegrini, M. J. Manfra, G. C. Gardner, L. N. Pfeiffer, and K. W. West, Observation of electron states of small period artificial graphene in nano-patterned GaAs quantum wells, Appl. Phys. Lett. **109**, 113101 (2016).

[18] S. Wang, D. Scarabelli, L. Du, Y. Y. Kuznetsova, L. N. Pfeiffer, K. W. West, G. C. Gardner, M. J. Manfra, V. Pellegrini, S. J. Wind, and A. Pinczuk, Observation of Dirac bands in artificial graphene in small-period nanopatterned GaAs quantum wells, Nat. Nanotechnol. **13**, 29 (2018).

[19] A. Taimi, A. P. Seitsonen, F. Baumberger, M. Hengsberger, Z.-X. Shen, T. Greber, and J. Osterwalder, Electronic structure at the C_{60}/metal interface: An angle-resolved photoemission and first-principles study, Phys. Rev. B **77**, 075134 (2008).

[20] W. W. Pai, H. T. Jeng, C.-M. Cheng, C.-H. Lin, X. Xiao, A. Zhao, X. Zhang, G. Xu, X. Q. Shi, M. A. Van Hove, C.-S. Hsue, and K.-D. Tsuei, Optimal Electron Doping of a C_{60} Monolayer on Cu(111) Via Interface Reconstruction, Phys. Rev. Lett. **104**, 036103 (2010).

[21] See Supplemental Material at http://link.aps.org/supplemental/10.1103/PhysRevB.102.201401 for experimental methods and analytical solution of the AG model.

[22] S. Modesti, S. Cerasari, and P. Rudolf, Determination of Charge States of C_{60} Adsorbed on Metal Surfaces, Phys. Rev. Lett. **71**, 2469 (1993).

[23] E. I. Altman and R. J. Colton, Nucleation, growth, and structure of fullerene films on Au(111), Surf. Sci. **279**, 49 (1992).

[24] L.-L. Wang and H.-P. Cheng, Density functional study of the adsorption of a C_{60} monolayer on Ag(111) and Au(111) surfaces, Phys. Rev. B **69**, 165417 (2004).

[25] I. Hamada and M. Tsukada, Adsorption of C_{60} on Au(111) revisited: A van der Waals density functional study, Phys. Rev. B **83**, 245437 (2011).

[26] P. K. Jain, X. Huang, I. H. El-Sayed, and M. A. El-Sayed, Review of some interesting surface plasmon resonance-enhanced properties of noble metal nanoparticles and their applications to biosystems, Plasmonics **2**, 107 (2007).

[27] L. Ju, B. Geng, J. Horng, C. Girit, M. Martin, Z. Hao, H. A. Bechtel, X. Liang, A. Zettl, Y. R. Shen, and F. Wang, Graphene plasmonics for tunable terahertz metamaterials, Nat. Nanotechnol. **6**, 630 (2011).

[28] J. Chen, M. Badioli, P. Alonso-González, S. Thongrattanasiri, F. Huth, J. Osmond, M. Spasenović, A. Centeno, A. Pesquera, P. Godignon, A. Zurutuza Elorza, N. Camara, F. J. G. de Abajo, R. Hillenbrand, and F. H. L. Koppens, Optical nano-imaging of gate-tunable graphene plasmons, Nature (London) **487**, 77 (2012).

[29] A. F. Hebard, M. J. Rosseinsky, R. C. Haddon, D. W. Murphy, S. H. Glarum, T. T. M. Palstra, A. P. Ramirez, and A. R. Kortan, Superconductivity at 18 K in potassium-doped C_{60}, Nature (London) **350**, 600 (1991).

[30] M.-Q. Ren, S. Han, S.-Z. Wang, J.-Q. Fan, C.-L. Song, X.-C. Ma, and Q.-K. Xue, Direct Observation of Full-Gap Superconductivity and Pseudogap in Two-Dimensional Fullerides, Phys. Rev. Lett. **124**, 187001 (2020).

[31] C. Cepek, I. Vobornik, A. Goldoni, E. Magnano, G. Selvaggi, J. Kröger, G. Panaccione, G. Rossi, and M. Sancrotti, Temperature-Dependent Fermi Gap Opening in the $c(6\times4)$-C_{60}/Ag(100) Two-Dimensional Superstructure, Phys. Rev. Lett. **86**, 3100 (2001).